Chapter 2
Characterizations of RF Tunable Devices

None of the RF tunable devices, such as BST varactors, SOI/SOS DTCs, and MEMS tunable capacitors, operating at radio or microwave frequency can be considered as an ideal lumped capacitor. They should be thought of two-port networks. The RF tunable devices, thus, need to be preliminarily characterized for determining their capacitance tuning region C_{max}/C_{min}, quality factor Q, and parasitics. There are no simple ways to directly measure these parameters.

The first two sections present the methodologies of characterizing a single device in series and shunt connecting configurations. The characterization will be directly from measured S-parameters to the extraction of component value without using middle step Y matrix as often used in previous work, such as in [1–6]. The third section describes the characterization of networks consisting of RF tunable devices.

2.1 Single Device Connected in Series

A single RF tunable device is mounted on a substrate and it is configured in series. In this case, this device can be generally characterized by a pi-network as illustrated in Fig. 2.1. Where the series impedance Z_S and the shunt admittances Y_1 and Y_2 can be expressed as

$$Z_S(\omega) = R_S(\omega) + jX_S(\omega) \tag{2.1}$$

$$Y_1(\omega) = G_1(\omega) + jB_1(\omega) \tag{2.2}$$

and

$$Y_2(\omega) = G_2(\omega) + jB_2(\omega) \tag{2.3}$$

Q. Gu, *RF Tunable Devices and Subsystems: Methods of Modeling, Analysis, and Applications*, DOI 10.1007/978-3-319-09924-8_2

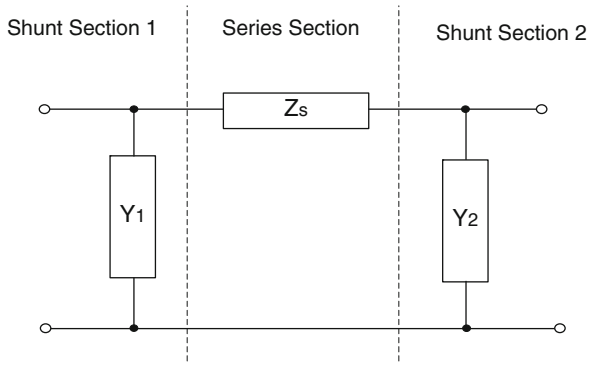

Fig. 2.1 Equivalent pi-network

where X_s and R_s are the reactance and resistance portions of the series impedance Z_s, B_i, and G_i ($i = 1, 2$) are the susceptance and conductance portions of the shunt admittance Y_i ($i = 1, 2$) at the input port and the output port of the equivalent circuit, respectively, and $\omega = 2\pi f$.

The series component Z_S determines the main function of the device under the characterization, and the shunt components, Y_1 and Y_2, represent the parasitics in the device. Z_S, Y_1, and Y_2 can be determined through measuring the S-parameters of the device. The relationships between Z_S/Y_i ($i = 1, 2$) and the corresponding S-parameters can be derived as follows.

Figure 2.1 pi-network can be considered as constituted by three two-port networks, two networks having a shunt admittance Y_i ($i = 1, 2$), respectively, and one network having a series impedance Z_S. These three simple networks are connected in cascade. The ABCD matrix characterizing the pi-network can be obtained by multiplying three individual ABCD matrixes of the simple networks in original cascaded order as expressed in (2.4).

$$\begin{aligned}\begin{bmatrix} A & B \\ C & D \end{bmatrix}_{pi} &= \begin{bmatrix} A_1 & B_1 \\ C_1 & D_1 \end{bmatrix}_{shunt\_1} \begin{bmatrix} A_S & B_S \\ C_S & D_S \end{bmatrix}_{series} \begin{bmatrix} A_2 & B_2 \\ C_2 & D_2 \end{bmatrix}_{shunt\_2} \\ &= \begin{bmatrix} 1 & 0 \\ Y_1 & 1 \end{bmatrix} \cdot \begin{bmatrix} 1 & Z_S \\ 0 & 1 \end{bmatrix} \cdot \begin{bmatrix} 1 & 0 \\ Y_2 & 1 \end{bmatrix} = \begin{bmatrix} 1 + Y_2 Z_S & Z_S \\ Y_1 + Y_2 + Y_1 Y_2 Z_S & 1 + Y_1 Z_S \end{bmatrix}\end{aligned} \tag{2.4}$$

The conversion formulas from ABCD matrix to S-parameter matrix for a two-port network are given in (2.5)–(2.9) [7].

$$S_{11} = \frac{AZ_o + B - CZ_o^2 - DZ_o}{\Delta} \tag{2.5}$$

$$S_{12} = \frac{2(AD - BC)Z_o}{\Delta} = \frac{2Z_o}{\Delta} \quad \text{since } AD - BC = 1 \tag{2.6}$$

$$S_{21} = \frac{2Z_o}{\Delta} \tag{2.7}$$

and

$$S_{22} = \frac{-AZ_o + B - CZ_o^2 + DZ_o}{\Delta} \tag{2.8}$$

where

$$\Delta = AZ_o + B + CZ_o^2 + DZ_o \tag{2.9}$$
$$Z_o = 50\,\Omega$$

Substituting A, B, C, and D elements in (2.4) into (2.5)–(2.9) and after manipulating, the S-parameters of Fig. 2.1 pi-network are expressed as

$$S_{11} = \frac{-\left(\overline{Y_1} + \overline{Y_2}\right) + \left[1 + \left(\overline{Y_2} - \overline{Y_1}\right) - \overline{Y_1 Y_2}\right] \cdot \overline{Z_S}}{2 + \overline{Y_1} + \overline{Y_2} + \left(1 + \overline{Y_1} + \overline{Y_2} + \overline{Y_1 Y_2}\right) \cdot \overline{Z_S}} \tag{2.10}$$

$$S_{12} = S_{21} = \frac{2}{2 + \overline{Y_1} + \overline{Y_2} + \left(1 + \overline{Y_1} + \overline{Y_2} + \overline{Y_1 Y_2}\right) \cdot \overline{Z_S}} \tag{2.11}$$

and

$$S_{22} = \frac{-\left(\overline{Y_1} + \overline{Y_2}\right) + \left[1 - \left(\overline{Y_2} - \overline{Y_1}\right) - \overline{Y_1 Y_2}\right] \cdot \overline{Z_S}}{2 + \overline{Y_1} + \overline{Y_2} + \left(1 + \overline{Y_1} + \overline{Y_2} + \overline{Y_1 Y_2}\right) \cdot \overline{Z_S}} \tag{2.12}$$

where

$$\overline{Z_S} = \frac{Z_S}{Z_o}, \quad \overline{Y_1} = Y_1 \cdot Z_o, \quad \text{and} \quad \overline{Y_2} = Y_2 \cdot Z_o \tag{2.13}$$

The next step is to solve equations (2.10)–(2.12) with three variables, $\overline{Y_1}$, $\overline{Y_2}$ and $\overline{Z_S}$. The final solutions are $\overline{Y_1}$, $\overline{Y_2}$ and $\overline{Z_S}$ expressed by the S-parameters, S_{11}, S_{21}, and S_{22}, which should result from device measurements.

Rearranging (2.11), we have (2.14), i.e., the denominator of (2.10)–(2.12) right side is equal to $2/S_{21}$.

$$2 + \overline{Y_1} + \overline{Y_2} + \left(1 + \overline{Y_1} + \overline{Y_2} + \overline{Y_1 Y_2}\right) \cdot \overline{Z_S} = \frac{2}{S_{21}} \tag{2.14}$$

Substituting (2.14) into (2.10) and (2.12), respectively, we obtain equations (2.15) and (2.16).

$$-\left(\overline{Y_1}+\overline{Y_2}\right)+\left[1+\left(\overline{Y_2}-\overline{Y_1}\right)-\overline{Y_1Y_2}\right]\cdot\overline{Z_S}=\frac{2S_{11}}{S_{21}} \tag{2.15}$$

and

$$-\left(\overline{Y_1}+\overline{Y_2}\right)+\left[1-\left(\overline{Y_2}-\overline{Y_1}\right)-\overline{Y_1Y_2}\right]\cdot\overline{Z_S}=\frac{2S_{22}}{S_{21}} \tag{2.16}$$

Adding (2.15) and (2.16) on both sides, we have (2.17)

$$\left(1-\overline{Y_1Y_2}\right)\cdot\overline{Z_S}-\left(\overline{Y_1}+\overline{Y_2}\right)=\frac{S_{11}+S_{22}}{S_{21}} \tag{2.17}$$

Then making addition of (2.14) with (2.15) and (2.16), respectively, we derive equations (2.18) and (2.19).

$$\left(1+\overline{Y_2}\right)\cdot\overline{Z_S}+1=\frac{1+S_{11}}{S_{21}} \tag{2.18}$$

and

$$\left(1+\overline{Y_1}\right)\cdot\overline{Z_S}+1=\frac{1+S_{22}}{S_{21}} \tag{2.19}$$

From (2.18) and (2.19) we can express $\overline{Y_1}$ and $\overline{Y_2}$ as a function of $\overline{Z_S}$.

$$\overline{Y_1}=\frac{1+S_{22}-S_{21}\left(1+\overline{Z_S}\right)}{S_{21}\overline{Z_S}} \tag{2.20}$$

and

$$\overline{Y_2}=\frac{1+S_{11}-S_{21}\left(1+\overline{Z_S}\right)}{S_{21}\overline{Z_S}} \tag{2.21}$$

Finally, we solve equation set (2.17)–(2.19) by plugging (2.20) and (2.21) into (2.17), and $\overline{Z_S}$ has a solution as

$$\overline{Z_S}=\frac{1+S_{11}+S_{22}+S_{11}S_{22}-S_{21}^2}{2S_{21}} \tag{2.22}$$

Substituting (2.22) into (2.20)–(2.22), we have $\overline{Y_1}$ and $\overline{Y_2}$ solutions, (2.23) and (2.24), respectively.

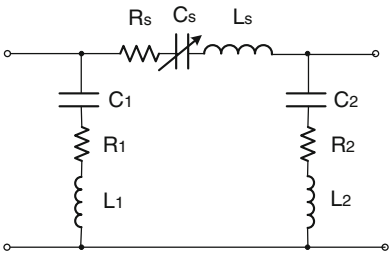

Fig. 2.2 Equivalent pi-network consisting of lumped components

$$\overline{Y_1} = \frac{1 + S_{22} - S_{11} - 2S_{21} - \left(S_{11}S_{22} - S_{21}^2\right)}{1 + S_{11} + S_{22} + \left(S_{11}S_{22} - S_{21}^2\right)} \tag{2.23}$$

and

$$\overline{Y_2} = \frac{1 + S_{11} - S_{22} - 2S_{21} - \left(S_{11}S_{22} - S_{21}^2\right)}{1 + S_{11} + S_{22} + \left(S_{11}S_{22} - S_{21}^2\right)} \tag{2.24}$$

The solutions given in (2.22)–(2.24) are normalized to $Z_o = 50\,\Omega$. The un-normalized Y_1, Y_2, and Z_S results are as follows.

$$\begin{aligned} Y_1 &= \frac{\overline{Y_1}}{Z_o} = G_1 + jB_1, \quad Y_2 = \frac{\overline{Y_2}}{Z_o} = G_2 + jB_2, \quad \text{and} \\ Z_S &= \overline{Z_S} \cdot Z_o = R_S + jX_S \end{aligned} \tag{2.25}$$

Using a pi-network to describe a series RF tunable device is more intuitive than directly using a measured S matrix. However, the pi-network with components expressed in impedance Z_s and admittance Y_i ($i = 1, 2$) is still not the best form for the circuit design.

A more proper way to represent the series RF tunable device is the pi-network with equivalent lumped components as shown in Fig. 2.2. Where C_S and R_S truly represent the series capacitor bank and the rests are parasitics caused by the interconnections and the package. The lumped components can be approximately considered as frequency independent in certain frequency range, say up to 2.2 GHz, which depends upon the complicity, size, and package form of the RF tunable devices. In this case, all the lumped components in Fig. 2.2 can be determined by measured S-parameters and (2.22)–(2.25) as follows.

The capacitors and parasitic inductors, C_k and L_k ($k = S, 1, 2$), can be obtained through measuring the S-parameters of the series device at a low-frequency f_L and a high-frequency f_H, and using the following reactance X_k ($k = S, 1, 2$) formulas.

$$X_S(\omega) = Z_o \mathrm{Im}\left(\frac{2S_{21}}{1 + S_{11} + S_{22} + S_{11}S_{22} - S_{21}^2}\right) \tag{2.26}$$

$$X_1(\omega) = Z_o \mathrm{Im}\left(\frac{1}{\overline{Y}_1}\right) = Z_o \mathrm{Im}\left(\frac{1 + S_{11} + S_{22} + \left(S_{11}S_{22} - S_{21}^2\right)}{1 + S_{22} - S_{11} - 2S_{21} - \left(S_{11}S_{22} - S_{21}^2\right)}\right) \tag{2.27}$$

and

$$X_2(\omega) = Z_o \mathrm{Im}\left(\frac{1}{\overline{Y}_2}\right) = Z_o \mathrm{Im}\left(\frac{1 + S_{11} + S_{22} + \left(S_{11}S_{22} - S_{21}^2\right)}{1 + S_{11} - S_{22} - 2S_{21} - \left(S_{11}S_{22} - S_{21}^2\right)}\right) \tag{2.28}$$

where $\omega = 2\pi f$ and Im $(\cdot)$ means the imaginary part of $(\cdot)$. The capacitors and inductors, C_k and L_k $(k = S, 1, 2)$, can be calculated by (2.29) and (2.30).

$$C_k = \frac{\omega_L^2 - \omega_H^2}{\omega_L \omega_H} \cdot \frac{1}{\omega_H X_k(\omega_L) - \omega_L X_k(\omega_H)} \tag{2.29}$$

and

$$L_k = \frac{\omega_L X_k(\omega_L) - \omega_H X_k(\omega_H)}{\omega_L^2 - \omega_H^2} \tag{2.30}$$

where $\omega_L = 2\pi f_L$ and $\omega_H = 2\pi f_H$. The capacitors and the inductors are approximately frequency independent in a certain frequency band, but the resistors R_k $(k = S, 1, 2)$ may be frequency dependent and R_S is capacitor value dependent as well. The resistors R_k $(k = S, 1, 2)$ can be calculated by employing the formulas (2.31)–(2.33).

$$R_S(\omega) = Z_o \cdot \mathrm{Re}\left(\frac{1 + S_{11} + S_{22} + S_{11}S_{22} - S_{21}^2}{2S_{21}}\right) \tag{2.31}$$

$$R_1(\omega) = Z_o \cdot \mathrm{Re}\left(\frac{1 + S_{11} + S_{22} + \left(S_{11}S_{22} - S_{21}^2\right)}{1 + S_{22} - S_{11} - 2S_{21} - \left(S_{11}S_{22} - S_{21}^2\right)}\right) \tag{2.32}$$

and

$$R_2(\omega) = Z_o \cdot \mathrm{Re}\left(\frac{1 + S_{11} + S_{22} + \left(S_{11}S_{22} - S_{21}^2\right)}{1 + S_{11} - S_{22} - 2S_{21} - \left(S_{11}S_{22} - S_{21}^2\right)}\right) \tag{2.33}$$

where Re$(\cdot)$ is the real part of $(\cdot)$. The resistance will be very small for high Q devices, and their accuracy strongly depends upon the accuracy of the S-parameter measurements.

Table 2.1 Measured S-parameters of a nominal 8 pF tunable capacitor and calculated Zs, Y_1, and Y_2

Freq. (GHz)	Re(S11)	Im(S11)	Re (S21)	Im(S21)	Re(S22)	Im(S22)	Zs	Y1	Y2
0.6	−0.074	−0.5235	0.8468	−0.01895	0.0538	−0.52705	0.1555–i29.7364	2.873E − 5 + i0.0086	−2.568E − 5 + i0.0035
1.6	−0.5065	−0.5161	0.5057	−0.4534	−0.46843	−0.55308	0.1735–i4.2342	0.0010 + i0.0290	−0.0005 + i0.0106

The measured S-parameters from a prototype MEMS tunable capacitor consisting of seven 1 pF composite cells and each of 1/8, 1/4, and 1/2 pF cells in all cells on-state and at frequency 0.6 and 1.6 GHz, respectively, are given in Table 2.1. In this table, the right three columns are calculation results of utilizing (2.22)–(2.25). The components of Fig. 2.2 in this device at its all cells on-state can be calculated from Table 2.2 and (2.26)–(2.33) by using the Excel spreadsheet.

$$C_S = 8.09\ \text{pF}, \quad L_S = 0.80\ \text{nH}, \quad \text{and} \quad R_S = 0.16\tilde{}0.18\ \Omega$$
$$C_1 = 2.19\ \text{pF}, \quad L_1 = 1.08\ \text{nH}, \quad \text{and} \quad R_1 = 0.39\tilde{}1.19\ \Omega$$
$$C_2 = 0.90\ \text{pF}, \quad L_2 = 1.63\ \text{nH}, \quad \text{and} \quad R_2 = 0.31\tilde{}0.09\ \Omega$$

At the off-state, the calculated C_S and L_S values of this device are 0.91 pF and 0.82 nH, respectively. The tuning ratio of this prototype tunable capacitor, C_{max}/C_{min}, is close to 9:1. The characterization accuracy heavily depends upon the precision of the device S-parameter measurements and de-embeddings.

The Q factor of the series tunable capacitor at the measurement frequency ω is

$$Q_C = \frac{1}{\omega C_S \cdot R_S} \tag{2.34}$$

The R_S is approximately 0.17 Ω at frequency 1 GHz, the Q factor of the above device at its on-state is approximately equal to

$$Q_C = \frac{1}{2\pi \cdot 10^9 \cdot 8.1 \cdot 10^{-12} \cdot 0.17} = 115.6.$$

We should notice that R_S is the loss resulting from both C_S and parasitic L_S. Equation (2.34) may be accurate only if the loss of L_S is much smaller than that of C_S. The Q factor of the device may also be determined by direct measurement of a parallel resonate circuit consisting of a high Q inductor and an RF tunable capacitor. The Q factor of the parasitics can be estimated based on the type of interconnection lines and the package structure.

If the L and C components in Fig. 2.2 are considered as lossy components and their loss is characterized by their Q factor:

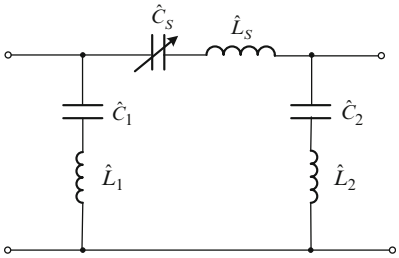

Fig. 2.3 Equivalent pi-network with lumped L and C having finite Q factor

$$\hat{C}_k = C_k\left(1 - \frac{j}{Q_{Ck}(f)}\right) \quad k = s,\ 1,\ 2 \tag{2.35}$$

and

$$\hat{L}_k = L_k\left(1 - \frac{j}{Q_{Ck}(f)}\right) \quad k = s,\ 1,\ 2 \tag{2.36}$$

The resistors in Fig. 2.2 are absorbed by C and L and the equivalent pi-network with lumped components turns into Fig. 2.3.

The frequency independent lumped components of the equivalent pi-network obtained from the above method are approximate. The more accurate equivalent pi-network with lumped components can be developed by using a circuit modeling approach discussed in Chap. 3.

2.2 Single Device Connected in Shunt

An RF tunable device is quite often used in shunt connection. In this case, the shunt device can be characterized by employing a T-network as depicted in Fig. 2.4. Where the series impedance Z_1 and Z_2 and the shunt admittances Y_{sh} can be expressed as

$$Z_1(\omega) = R_1(\omega) + jX_1(\omega) \tag{2.37}$$

$$Z_2(\omega) = R_2(\omega) + jX_2(\omega) \tag{2.38}$$

and

$$Y_{Sh}(\omega) = G_{Sh}(\omega) + jB_{Sh}(\omega) \tag{2.39}$$

where X_i and R_i (i = 1, 2) are the reactance and resistance portions of Z_i (i = 1, 2), B_{Sh} and G_{Sh} are the suspectance and conductance portions of Y_{Sh}, and $\omega = 2\pi f$.

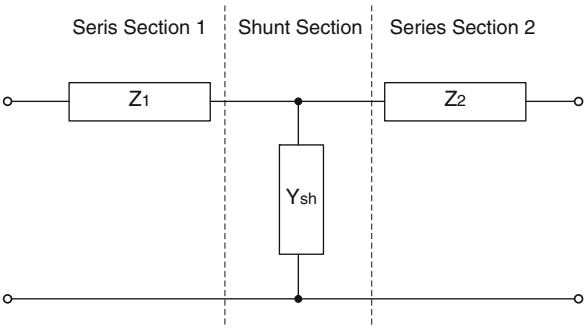

Fig. 2.4 Equivalent T-network of a shunt capacitor banks

Using the same derivation approach as presented in Sect. 2.1 we can obtain the following expressions (2.40)–(2.42).

$$\overline{Y_{Sh}} = \frac{1 - S_{11} - S_{22} + S_{11}S_{22} - S_{21}^2}{2S_{21}} \tag{2.40}$$

$$\overline{Z_1} = \frac{1 + S_{11} - S_{22} - 2S_{21} - \left(S_{11}S_{22} - S_{21}^2\right)}{1 - S_{11} - S_{22} + \left(S_{11}S_{22} - S_{21}^2\right)} \tag{2.41}$$

and

$$\overline{Z_2} = \frac{1 - S_{11} + S_{22} - 2S_{21} - \left(S_{11}S_{22} - S_{21}^2\right)}{1 - S_{11} - S_{22} + \left(S_{11}S_{22} - S_{21}^2\right)} \tag{2.42}$$

where $\overline{Z_1}$, $\overline{Z_2}$ and $\overline{Y_{Sh}}$ are normalized Z_1, Z_2, and Y_{Sh} by $Z_o = 50\,\Omega$, respectively. Z_1, Z_2, and Y_{Sh} can be derived as shown in (2.41).

$$\begin{aligned} Z_1 = \overline{Z_1}Z_o = R_1 + jX_1, \quad Z_2 = \overline{Z_2}Z_o = R_2 + jX_2, \quad \text{and} \quad Y_{Sh} = \frac{\overline{Y_{Sh}}}{Z_o} \\ = G_{Sh} + jB_{Sh} \end{aligned} \tag{2.43}$$

The admittance Y_{Sh} in the T-network plays the main function of the shunt RF tunable device, and impedance Z_i (i = 1, 2) are the parasitics. The susceptance B_{Sh} and the reactance X_1 and X_2 in (2.37)–(2.39) have forms as

$$B_{Sh}(\omega) = \frac{1}{Z_o}\mathrm{Im}\left(\frac{1 - S_{11} - S_{22} + S_{11}S_{22} - S_{21}^2}{2S_{21}}\right) \tag{2.44}$$

$$X_1(\omega) = Z_o \mathrm{Im}\left(\frac{1 + S_{11} - S_{22} - 2S_{21} - \left(S_{11}S_{22} - S_{21}^2\right)}{1 - S_{11} - S_{22} + \left(S_{11}S_{22} - S_{21}^2\right)}\right) \tag{2.45}$$

and

$$X_2(\omega) = Z_o \mathrm{Im}\left(\frac{1 - S_{11} + S_{22} - 2S_{21} - \left(S_{11}S_{22} - S_{21}^2\right)}{1 - S_{11} - S_{22} + \left(S_{11}S_{22} - S_{21}^2\right)}\right) \tag{2.46}$$

The conductance G_{Sh} and the resistance R_1 and R_2 have expressions (2.47)–(2.49).

$$G_{Sh}(\omega) = \frac{1}{Z_o}\mathrm{Re}\left(\frac{1 - S_{11} - S_{22} + S_{11}S_{22} - S_{21}^2}{2S_{21}}\right) \tag{2.47}$$

$$R_1(\omega) = Z_o \mathrm{Re}\left(\frac{1 + S_{11} - S_{22} - 2S_{21} - \left(S_{11}S_{22} - S_{21}^2\right)}{1 - S_{11} - S_{22} + \left(S_{11}S_{22} - S_{21}^2\right)}\right) \tag{2.48}$$

and

$$R_2(\omega) = Z_o \mathrm{Re}\left(\frac{1 - S_{11} + S_{22} - 2S_{21} - \left(S_{11}S_{22} - S_{21}^2\right)}{1 - S_{11} - S_{22} + \left(S_{11}S_{22} - S_{21}^2\right)}\right) \tag{2.49}$$

The lumped component form of Fig. 2.4 equivalent T-network is shown in Fig. 2.5. The network with lumped components is more intuitive than the network with the impedance and admittance. It is also favorable for the circuit design.

As described in the previous subsection, the lumped components in the equivalent network of the device can be obtained from the measured S-parameters at a low-frequency f_L and a high-frequency f_H and calculations of formulas, such as (2.29). For the components in Fig. 2.5, we may use (2.50) and (2.51).

$$C_{Sh} = \frac{\omega_L^2 - \omega_H^2}{\omega_L \omega_H} \cdot \frac{1}{\omega_H X_{Sh}(\omega_L) - \omega_L X_{Sh}(\omega_H)} \tag{2.50}$$

and

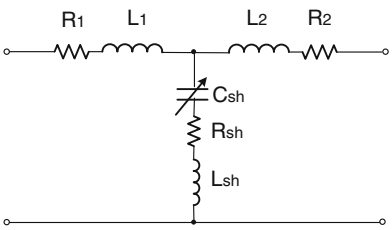

Fig. 2.5 Equivalent T-network with lumped components

$$L_{Sh} = \frac{\omega_L X_{Sh}(\omega_L) - \omega_H X_{Sh}(\omega_H)}{\omega_L^2 - \omega_H^2} \tag{2.51}$$

where

$$X_{Sh}(\omega) = Z_o \mathrm{Im}\left(\frac{1}{\overline{Y}_{Sh}}\right) = Z_o \mathrm{Im}\left(\frac{2S_{21}}{1 - S_{11} - S_{22} + S_{11}S_{22} - S_{21}^2}\right) \tag{2.52}$$

The other lumped components in Fig. 2.5 can be approximately obtained by using the following expressions.

$$L_1 = \frac{Z_o}{\omega} \mathrm{Im}\left(\frac{1 + S_{11} - S_{22} - 2S_{21} - \left(S_{11}S_{22} - S_{21}^2\right)}{1 - S_{11} - S_{22} + \left(S_{11}S_{22} - S_{21}^2\right)}\right) \tag{2.53}$$

$$L_2 = \frac{Z_o}{\omega} \mathrm{Im}\left(\frac{1 - S_{11} + S_{22} - 2S_{21} - \left(S_{11}S_{22} - S_{21}^2\right)}{1 - S_{11} - S_{22} + \left(S_{11}S_{22} - S_{21}^2\right)}\right) \tag{2.54}$$

$$R_{Sh}(\omega) = Z_o \mathrm{Re}\left(\frac{2S_{21}}{1 - S_{11} - S_{22} + S_{11}S_{22} - S_{21}^2}\right) \tag{2.55}$$

$$R_1(\omega) = Z_o \mathrm{Re}\left(\frac{1 + S_{11} - S_{22} - 2S_{21} - \left(S_{11}S_{22} - S_{21}^2\right)}{1 - S_{11} - S_{22} + \left(S_{11}S_{22} - S_{21}^2\right)}\right) \tag{2.56}$$

and

$$R_2(\omega) = Z_o \mathrm{Re}\left(\frac{1 - S_{11} + S_{22} - 2S_{21} - \left(S_{11}S_{22} - S_{21}^2\right)}{1 - S_{11} - S_{22} + \left(S_{11}S_{22} - S_{21}^2\right)}\right) \tag{2.57}$$

A tunable capacitor comprises two capacitor banks. One capacitor bank contains seven 1 pF two-state composite capacitor cells and another one consists of 1/8, 1/4, and 1/2 pF two-state capacitor cells. The total nominal capacitance of each capacitor bank should be 7 and 7/8 pF. These two capacitor banks are connected together and both are configured in shunt. The measured S-parameters from this tunable capacitor in all capacitor banks on-state at frequencies 0.5 and 1.0 GHz are presented in Table 2.2. The calculated impedance Z_k ($k = \mathrm{Sh}, 1, 2$) from (2.40)–(2.43) are also shown in Table 2.2.

Table 2.2 Measured S-parameters of a 15¾ pF tunable capacitor and calculated Z_{Sh}, Z_1, and Z_2

Freq. (GHz)	Re(S11)	Im(S11)	Re(S21)	Im(S21)	Re(S22)	Im(S22)	Z_{sh}	Z_1	Z_2
0.5	−0.658895	−0.45123	0.336967	−0.49253	−0.66157	−0.4475581	0.0550–i18.3917	0.0010 + i0.0202	0.0009 + i0.0230
1.0	−0.888393	−0.2542	0.10162	−0.352	−0.88922	−0.2510076	0.0365–i8.9897	0.0023 + i0.0492	−0.0023 + i0.0509

Utilizing (2.50)–(2.57), we can determine the lumped components in Fig. 2.7 T-network, and when the tunable capacitor is in all cells on-state, they are

$$C_{Sh} = 17.18 \text{ pF}, \quad L_S = 0.043 \text{ nH}, \quad \text{and} \quad R_S = 0.049\tilde{}0.046\ \Omega$$
$$L_1 = 0.39 \text{ nH}, \quad \text{and} \quad R_1 = 0.05\tilde{}0.11\ \Omega$$
$$L_2 = 0.40 \text{ nH}, \quad \text{and} \quad R_2 = 0.04\tilde{}0.12\ \Omega$$

The lumped component value at the tunable capacitor off-state can be derived by adopting the same approach as described above.

The Q factor of a shunt capacitor bank at frequency ω has the expression as (2.58).

$$Q_C = \frac{1}{\omega \cdot C_{Sh} \cdot R_{Sh}} \tag{2.58}$$

The Q factor of the above tunable capacitor in its on-state at frequency 1 GHz is approximately equal to

$$Q_C = \frac{1}{2\pi \cdot 10^9 \cdot 17.2 \cdot 10^{-12} \cdot 0.046} = 201.4.$$

The Q factor of the RF tunable capacitor bank can be determined by using a resonate circuit consisting of a high Q inductor and an RF tunable capacitor bank. The Q factor of the parasitics can be estimated based on the type of interconnection lines and the package structure.

If using finite Q factor of capacitor C and inductor L with expressions given in (2.35) and (2.36), the equivalent T-network Fig. 2.5 turns into Fig. 2.6.

The frequency independent lumped components derived in this section are approximate. The more accurate equivalent T-network with lumped components can be obtained by using a circuit modeling approach given in Chap. 3.

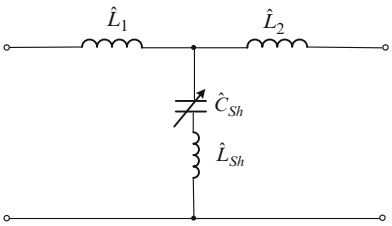

Fig. 2.6 Equivalent T-network with lumped components having finite Q factor

2.3 A Network Consisting of RF Tunable Capacitors

In this section, the characterization methods of a network consisting RF tunable capacitors will discussed, The network is configured by the tunable capacitors integrated on the same chip in a single package. The tunable capacitors can consist of BST varactors, SOI/SOS DTCs, or MEMS tunable capacitor banks. There are two cases addressed in this section. A network contains the tunable capacitors only and external inductors need to be used. The characterization of the network without integrated inductors is presented in Sect. 2.3.1. Another network has integrated inductors and its characterization will be more complicated than the previous one. The characterization approach for the latter one is described in Sect. 2.3.2.

2.3.1 A Network Without Integrated Inductors

A network contains four tunable capacitors C_i ($i = 1$, 2, 3, and 4) and they are configured in a capacitor-bridged double pi-network [8] as shown in Fig. 2.7a. The capacitance value of the four capacitors can be obtained through measuring the S-parameters of the network at a low frequency and using formula (2.59)–(2.61) in Sect. 2.1 as follows.

$$C_1 = \frac{-Z_o}{\omega} \cdot \mathrm{Im}\left(\frac{1 + S_{11} + S_{22} + \left(S_{11}S_{22} - S_{21}^2\right)}{1 + S_{22} - S_{11} - 2S_{21} - \left(S_{11}S_{22} - S_{21}^2\right)} \right) \tag{2.59}$$

$$C_2 = \frac{-Z_o}{\omega} \cdot \mathrm{Im}\left(\frac{1 + S_{11} + S_{22} + \left(S_{11}S_{22} - S_{21}^2\right)}{1 + S_{11} - S_{22} - 2S_{21} - \left(S_{11}S_{22} - S_{21}^2\right)} \right) \tag{2.60}$$

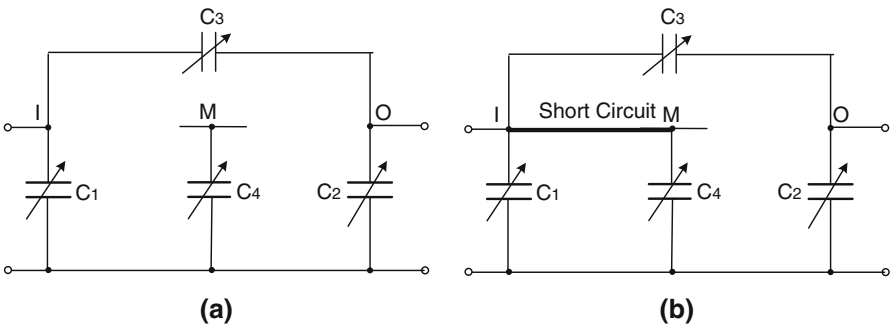

Fig. 2.7 A capacitor-bridged double pi-network

and

$$C_3 = \frac{-Z_o}{\omega} \cdot \mathrm{Im}\left(\frac{2S_{21}}{1 + S_{11} + S_{22} + S_{11}S_{22} - S_{21}^2}\right) \tag{2.61}$$

- First, measure the S-parameters of Fig. 2.7a at a low frequency, say 100 MHz, with I and O nodes as input and output ports.
- Use the measured S-parameters and (2.59), (2.60), and (2.61) to calculate C_1, C_2, and C_3, respectively.
- Secondly, measure the S-parameters of Fig. 2.7b with nodes I and M connected together at the same frequency.
- Use the second time measured S-parameters and formula (2.59) to recalculate $C_{1,4}$, where

$$C_{1,4} = C_1 + C_4 \tag{2.62}$$

- Finally, the middle C_4 is obtained from $C_{1,4}$ minus C_1, i.e.,

$$C_4 = C_{1,4} - C_1 \tag{2.63}$$

The procedure of the capacitor value determination explained in an intuitive plot is shown in Fig. 2.8. An example of that Excel spreadsheet calculation results are depicted in Table 2.3.

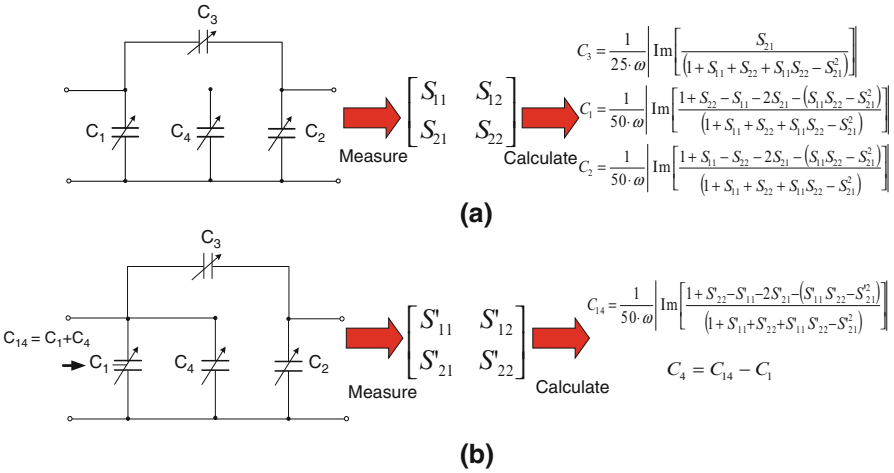

Fig. 2.8 Determination procedure of bank capacitance in a capacitor-bridged double pi-network without integrated inductor

Table 2.3 Example of Excel spreadsheet calculation for bank capacitance in Fig. 2.7a

Input Data Area									Output Data Area					
Freq (Hz)	S11 mag	S11 phase	S21 mag	S21 phase	S12 mag	S12 phase	S22 mag	S22 phase	G3 (μS)	C3 (pF)	G1 (μS)	C1 (pF)	G2(μS)	C2 (pF)
1.00E+08	0.98382	-27.9891	0.175896	61.94658	0.175896	61.94658	0.98382	-27.9891	2.36	3.00	3.94	5.00	3.94	5.00
1.02E+08	0.983247	-28.5176	0.178938	61.41716	0.178938	61.41716	0.983256	-28.5173	2.46	3.00	4.14	5.00	4.04	5.00
1.04E+08	0.982665	-29.0443	0.181954	60.88943	0.181954	60.88943	0.982674	-29.044	2.56	3.00	4.35	5.00	4.26	5.00
1.06E+08	0.982084	-29.569	0.184945	60.36329	0.184945	60.36329	0.982098	-29.5692	2.66	3.00	4.51	5.00	4.37	5.00
1.08E+08	0.98149	-30.0927	0.18791	59.83895	0.18791	59.83895	0.981512	-30.0926	2.76	3.00	4.78	5.00	4.54	5.00
1.10E+08	0.980903	-30.6142	0.190849	59.31659	0.190849	59.31659	0.980916	-30.6145	2.86	3.00	4.93	5.00	4.78	5.00
Input Data Area									Output Data Area					
Freq (Hz)	S11 mag	S11 phase	S21 mag	S21 phase	S12 mag	S12 phase	S22 mag	S22 phase	G14 (μS)	C14 (pF)	G1 (μS)	C1 (pF)	G4(μS)	C4 (pF)
1.00E+08	0.984655	-41.1017	0.169816	55.44056	0.169816	55.44056	0.984893	-27.8993	7.09	9.00	3.94	5.00	3.14	4.00
1.02E+08	0.98415	-41.8454	0.17253	54.80475	0.17253	54.80475	0.984397	-28.4236	7.38	9.00	4.14	5.00	3.24	4.00
1.04E+08	0.983646	-42.5844	0.175221	54.17457	0.175221	54.17457	0.983901	-28.9458	7.70	9.00	4.35	5.00	3.35	4.00
1.06E+08	0.983139	-43.3197	0.177867	53.54372	0.177867	53.54372	0.9834	-29.4666	7.98	9.00	4.51	5.00	3.46	4.00
1.08E+08	0.982624	-44.0512	0.180485	52.91995	0.180485	52.91995	0.982902	-29.9858	8.44	9.00	4.78	5.00	3.66	4.00
1.10E+08	0.982115	-44.7777	0.183067	52.2963	0.183067	52.2963	0.982401	-30.503	8.73	9.00	4.93	5.00	3.81	4.00

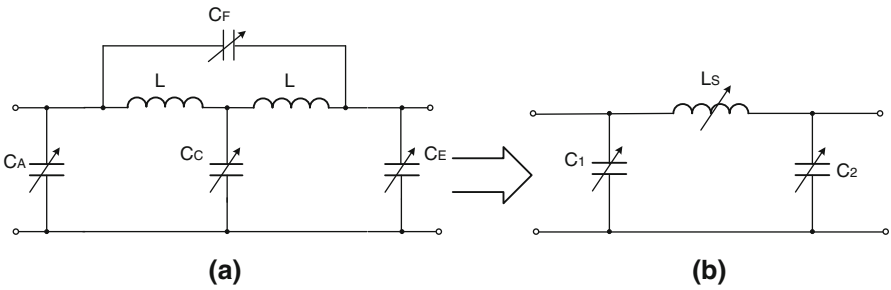

Fig. 2.9 Capacitor-bridged double pi-network (**a**) with integrated inductors L and equivalent pi-network (**b**)

2.3.2 *A Network with Integrated Inductors*

A capacitor-bridged double pi-network [8] with integrated inductors L is depicted in Fig. 2.9a. The C_{min} and C_{max} values of C_A, C_C, C_E, and C_F tunable capacitors and the inductance L in the network Fig. 2.9a can be obtained by means of the measurements of the network S-parameters and the component extractions from the equivalent pi-network. The components L_S, C_1, and C_2 in equivalent pi-network Fig. 2.9b have the following relationships with components C_A, C_C, C_E, C_F, and L.

$$C_1 = C_A + C_o = C_A + \frac{C_C}{2 - \omega^2 L C_C} \tag{2.64}$$

$$C_2 = C_E + C_o = C_E + \frac{C_C}{2 - \omega^2 L C_C} \tag{2.65}$$

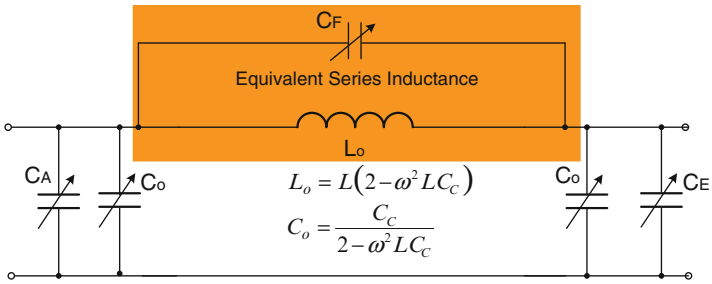

Fig. 2.10 Explicit form of equivalent pi-network Fig. 2.9b

and

$$L_S = \frac{L(2-\omega^2 LC_C)}{1-\omega^2 LC_F(2-\omega^2 LC_C)} \tag{2.66}$$

where $\omega = 2\pi f$ and f is the test frequency. The equivalent pi-network Fig. 2.9b can be explicitly expressed as Fig. 2.10.

2.3.2.1 Method of Determining $C_{C,Min}$, $C_{C,Max}$, $C_{F,Min}$, $C_{F,Max}$, and L

To have the values of C_A, C_C, C_E, and C_F capacitors and the inductance L in the network Fig. 2.9a, we first take the following steps of the S-parameters measurement at a low frequency, 10 ~ 100 MHz:

1. All bank capacitors Off: $C_{A,Min}$, $C_{C,Min}$, $C_{E,\,Min}$, and $C_{F,Min}$
   Pi network extraction → $C_{1,Min}$, $C_{2,Min}$, and $L_{S,Min}$
2. All bank capacitors On: $C_{A,Max}$, $C_{C,Max}$, $C_{E,\,Max}$, and $C_{F,Max}$
   Pi network extraction → $C_{1,Max}$, $C_{2,Max}$, and $L_{S,MaxFC}$
3. A bank capacitor On and all others Off: $C_{A,Max}$, $C_{C,Min}$, $C_{E,\,Min}$, and $C_{F,Min}$
   Pi network extraction → $C_{1,MaxA}$, $C_{2,Min}$, and $L_{S,Min}$
4. C bank capacitor On and all others Off: $C_{A,Min}$, $C_{C,Max}$, $C_{E,\,Min}$, and $C_{F,Min}$
   Pi network extraction → $C_{1,MaxC}$, $C_{2,MaxC}$, and $L_{S,MaxC}$
5. E bank capacitor On and all others Off: $C_{A,Min}$, $C_{C,Min}$, $C_{E,\,Max}$, and $C_{F,Min}$
   Pi network extraction → $C_{1,Min}$, $C_{2,MaxE}$, and $L_{S,\,Min}$
6. F bank capacitor On and all others Off: $C_{A,Min}$, $C_{C,Min}$, $C_{E,\,Min}$, and $C_{F,Max}$
   Pi network extraction → $C_{1,Min}$, $C_{2,Min}$, and $L_{S,MaxF}$

From these steps of measurements, we can obtain:

$$\Delta C_A = C_{1,MaxA} - C_{1,Min} \tag{2.67}$$

$$\Delta C_C = C_{1,MaxC} - C_{1,Min} + C_{2,MaxC} - C_{2,Min} \tag{2.68}$$

$$\Delta C_E = C_{2,MaxE} - C_{2,Min} \tag{2.69}$$

and

$$L_{S,Min}, L_{S,MaxFC}, L_{S,MaxC}, \quad \& \quad L_{S,MaxF} \tag{2.70}$$

where $L_{S,Min}$ approaches $2L$ (L, inductance of integrated inductors in the network, see Fig. 2.9a) when the $C_{C,Min}$ and $C_{F,Min}$ are small (say less than 0.5 pF) or testing frequency is low (say 50 MHz or lower). In determining $C_{C,Min}$, $C_{F,Min}$, and $C_{F,Max}$, we shall use the measurement data given in (2.70).

To get rid of as much parasitic influence as possible, ΔC_x ($x =$ A, C, and E) and $L_S = 2L$ measurements should be carried out at low frequency (say 50 MHz or lower). However, to determine C_C and C_F the measurement frequency needs to be high enough (say 800 MHz or 1 GHz) to make the equivalent inductance L_S difference being large enough for achieving accurate calculations when C_C and C_F take their minimum and/or maximum values.

In fact, $C_{C,Min}$ plays a important role in obtaining minimum and maximum values of A, C, and E capacitors. The $C_{C,Max}$ can be expressed as

$$C_{C,Max} = C_{C,Min} + \Delta C_C \tag{2.71}$$

$C_{A,Min}$ and $C_{E,\ Min}$ can be derived by substituting $C_{C,Min}$ into (2.64) and (2.65), respectively. When the test frequency is low, the term $\omega^2 L C_C$ and $\omega^2 L C_F$ in (2.64)–(2.66) can be neglected since they are much smaller than the tolerance of the measurements that can be reached. For example, $\omega^2 L C_C \cong 10^{-5}$ when $L = 2.5$ nH, $C_{C,Min} \leq 1$ pF, and $f = 10$ MHz. At low frequency, we have

$$C_1 = C_A + C_o = C_A + \frac{C_C}{2} \tag{2.72}$$

$$C_2 = C_E + C_o = C_E + \frac{C_C}{2} \tag{2.73}$$

and

$$L_S = 2L \ \text{ or } \ L = \frac{L_S}{2} \tag{2.74}$$

If $C_{C,Min}$ has been derived, utilizing (2.72) and (2.73) we can calculate $C_{A,Min}$ and $C_{E,\ Min}$ from (2.75) and (2.76).

$$C_{A,Min} = C_{1,Min} - \frac{C_{C,Min}}{2} \tag{2.75}$$

and

$$C_{E,Min} = C_{2,Min} - \frac{C_{C,Min}}{2} \tag{2.76}$$

From (2.67) and (2.69), we obtain the maximum values of C_A and C_E to be, respectively,

$$C_{A,Max} = C_{A,Min} + \Delta C_A = C_{A,Min} + C_{1,MaxA} - C_{1,Min} \tag{2.77}$$

$$C_{E,Max} = C_{E,Min} + \Delta C_E = C_{E,Min} + C_{2,MaxE} - C_{2,Min} \tag{2.78}$$

Now, we discuss the key derivation of obtaining $C_{C,Min}$, $C_{F,Min}$, and $C_{F,Max}$. In fact from the measurements and the extractions of the equivalent pi-network elements, based on (2.66) we can derive the following four equations, (2.79)–(2.82).

$$L_{S,Min} = \frac{L(2 - \omega^2 LC_{C,Min})}{1 - \omega^2 LC_{F,Min}(2 - \omega^2 LC_{C,Min})} \tag{2.79}$$

$$L_{S,MaxFC} = \frac{L[2 - \omega^2 L(C_{C,Min} + \Delta C_C)]}{1 - \omega^2 LC_{F,Max}[2 - \omega^2 L(C_{C,Min} + \Delta C_C)]} \tag{2.80}$$

$$L_{S,MaxC} = \frac{L[2 - \omega^2 L(C_{C,Min} + \Delta C_C)]}{1 - \omega^2 LC_{F,Min}[2 - \omega^2 L(C_{C,Min} + \Delta C_C)]} \tag{2.81}$$

and

$$L_{S,MaxF} = \frac{L(2 - \omega^2 LC_{C,Min})}{1 - \omega^2 LC_{F,Max}(2 - \omega^2 LC_{C,Min})} \tag{2.82}$$

Four equations, (2.79)–(2.82), can be used to solve four variables, $C_{C,Min}$, $C_{F,Min}$, $C_{F,Max}$, and L, but the L has been obtained from the low-frequency measurement and (2.74). We only need three equations, (2.79), (2.80) and (2.81), to obtain solutions of $C_{C,Min}$, $C_{F,Min}$, and $C_{F,Max}$. To simplify the forms of these equations, we introduce the following two intermediate parameters

$$\alpha = \omega^2 L^2 \tag{2.83}$$

and

$$x = L \cdot \left(2 - \omega^2 LC_{C,Min}\right) \tag{2.84}$$

Plugging (2.83) and (2.84) into (2.79) and (2.81),

$$L_{S,Min}\left(1 - \omega^2 C_{F,Min} x\right) = x \tag{2.85}$$

and

$$L_{S,MaxC}\left[1-\omega^2 C_{F,Min}(x-\alpha\cdot\Delta C_C)\right]=x-\alpha\cdot\Delta C_C \tag{2.86}$$

Manipulating (2.85), we can express $C_{F,Min}$ as

$$C_{F,Min}=\frac{L_{S,Min}-x}{\omega^2 L_{S,Min}x} \tag{2.87}$$

Substituting (2.87) into (2.86), we obtain equation (2.88) of x

$$x^2-\alpha\cdot\Delta C_C x-\frac{L_{S,Min}L_{S,MaxC}\alpha\cdot\Delta C_C}{L_{S,Min}-L_{S,MaxC}}=0 \tag{2.88}$$

The solution of (2.88) is

$$\begin{aligned} x&=\frac{\alpha\cdot\Delta C_C+\sqrt{(\alpha\cdot\Delta C_C)^2+4\dfrac{L_{S,Min}L_{S,MaxC}\alpha\Delta C_C}{L_{S,Min}-L_{S,MaxC}}}}{2}\\ &=\frac{\alpha\cdot\Delta C_C\left(1+\sqrt{1+4\dfrac{L_{S,Min}L_{S,MaxC}}{(L_{S,Min}-L_{S,MaxC})\cdot\alpha\cdot\Delta C_C}}\right)}{2} \end{aligned} \tag{2.89}$$

From (2.84), we drive $C_{C,Min}$ having a form of

$$C_{C,Min}=\frac{2L-x}{\alpha}=\frac{2}{\omega^2 L}-\frac{\Delta C_C\left(1+\sqrt{1+4\frac{L_{S,Min}L_{S,MaxC}}{\left(L_{S,Min}-L_{S,MaxC}\right)\cdot\alpha\cdot\Delta C_C}}\right)}{2} \tag{2.90}$$

$C_{C,Max}$ is simply expressed as

$$C_{C,Max}=C_{C,Min}+\Delta C_C \tag{2.91}$$

or from (2.80) and (2.82) we can drive $C_{C,Max}$ with a similar form as (2.90)

$$C_{C,Max}=\frac{2}{\omega^2 L}-\frac{\Delta C_C\left(-1+\sqrt{1+4\frac{L_{S,MaxF}L_{S,MaxFC}}{\left(L_{S,MiaxF}-L_{S,MaxFC}\right)\cdot\alpha\cdot\Delta C_C}}\right)}{2} \tag{2.92}$$

We can obtain $C_{F,Min}$ by substituting (2.83) into (2.81).

$$\begin{aligned} C_{F,Min}&=\frac{L_{S,Min}-x}{\omega^2 L_{S,Min}x}\\ &=\frac{2}{\omega^2\alpha\cdot\Delta C_C\left(1+\sqrt{1+4\frac{L_{S,Min}L_{S,MaxC}}{\left(L_{S,Min}-L_{S,MaxC}\right)\cdot\alpha\cdot\Delta C_C}}\right)}-\frac{1}{\omega^2 L_{S,Min}} \end{aligned} \tag{2.93}$$

Now we determine ΔC_F by using (2.79) and (2.82). Manipulating (2.79) and (2.82), we have

$$L_{S,Min}\left[1-\omega^2 LC_{F,Min}\left(2-\omega^2 LC_{C,Min}\right)\right]=L\left(2-\omega^2 LC_{C,Min}\right)$$
$$L_{S,MaxF}\left[1-\omega^2 LC_{F,Max}\left(2-\omega^2 LC_{C,Min}\right)\right]=L\left(2-\omega^2 LC_{C,Min}\right)$$

It is apparent that the left side of the above two equations is equal, and we obtain

$$\begin{aligned}&L_{S,Min}\left[1-\omega^2 LC_{F,Min}\left(2-\omega^2 LC_{C,Min}\right)\right]\\&\quad=L_{S,MaxF}\left[1-\omega^2 L(C_{F,Min}+\Delta C_F)\left(2-\omega^2 LC_{C,Min}\right)\right]\end{aligned}$$

This equation can be simplified as

$$\omega^2 L_{S,MaxF}L_{S,Min}\Delta C_F=L_{S,MaxF}-L_{S,Min}$$

Finally, we obtain the ΔC_F expression as

$$\Delta C_F=\frac{1}{\omega^2}\left(\frac{1}{L_{S,Min}}-\frac{1}{L_{S,MaxF}}\right) \tag{2.94}$$

From (2.80) and (2.81), we can derive another ΔC_F expression (2.95), which gives you the same results as (2.94)

$$\Delta C_F=\frac{1}{\omega^2}\left(\frac{1}{L_{S,MaxC}}-\frac{1}{L_{S,MaxFC}}\right) \tag{2.95}$$

In fact, we can directly derive $C_{F,Min}$ and $C_{F,Max}$ from (2.79)–(2.82) (see Appendix).

$$C_{F,Min}=\frac{-(L_{S,Min}+L_{S,MaxC})+\sqrt{(L_{S,Min}+L_{S,MaxC})^2-4L_{S,Min}\cdot L_{S,MaxC}\left(1-\frac{L_{S,Min}-L_{S,MaxC}}{\alpha\cdot\Delta C_C}\right)}}{2\omega^2 L_{S,Min}\cdot L_{S,MaxC}} \tag{2.96}$$

and

$$C_{F,Max}=\frac{-(L_{S,MaxF}+L_{S,MaxFC})+\sqrt{(L_{S,MaxF}+L_{S,MaxFC})^2-4L_{S,MaxF}\cdot L_{S,MaxFC}\left(1-\frac{L_{S,MaxF}-L_{S,MaxFC}}{\alpha\cdot\Delta C_C}\right)}}{2\omega^2 L_{S,MaxF}\cdot L_{S,MaxFC}} \tag{2.97}$$

It is apparent that we can calculate $C_{C,Min}$, $C_{C,Max}$, $C_{F,Min}$, and $C_{F,Max}$ from ΔC_C. The measurement of ΔC_C must be very accurate and it is carried out at low frequency (say 10 MHz). On the other hand, $C_{C,Min}$ and $C_{F,Min}$ values calculated from (2.90), (2.93), or (2.96) are very small. They are at 5×10^{-13} order and ΔC_C measurement error may cause unacceptable calculation errors on $C_{C,Min}$, $C_{C,Max}$, $C_{F,Min}$, and $C_{F,Max}$.

When we calculate $C_{C,Min}$, the corresponding $C_{A,Min}$ and $C_{E,Min}$ can be obtained from (2.75) and (2.76). $C_{A,Max}$ and $C_{E,Max}$, thus can be easily calculated by using (2.77) and (2.78). These measurements are better to be carried out at low frequency for achieving good accuracy without the frequency effect impact.

2.3.2.2 Calculation Example

In this subsection we use tested results of a capacitor-bridged double pi-network presented in Table 2.4 to calculate its $C_{C,Min}$, $C_{C,Max}$, $C_{F,Min}$, and $C_{F,Max}$. In this table, we have

$$L_{S,Min} = 4.17 \quad \text{nH} \tag{2.98a}$$

$$L_{S,MaxFC} = 6.14 \quad \text{nH} \tag{2.98b}$$

$$L_{S,MaxC} = 3.68 \quad \text{nH} \tag{2.98c}$$

$$L_{S,MaxF} = 7.65 \quad \text{nH} \tag{2.98d}$$

At present, we do not have a ΔC_C tested at low frequency, but we cannot use the calculated ΔC_C from Table 2.4. The calculated ΔC_C from Table 2.4 is usually higher than that obtained from the low-frequency measurement. In this case, we need to only use the spreadsheet to estimate ΔC_C and it is close to 2.73 pF. The series inductor L in this example is 2 nH each.

Substituting the L_S values given in (2.98a, 2.98b, 2.98c, and 2.98d) and estimated $\Delta C_C = 2.73$ pF into (2.90), we calculate $C_{C,Min}$

Table 2.4 A capacitor-bridged double pi-network test results (Test Frequency: 1 GHz)

	C1 (pF)	G1 (μmho)	Ls (nH)	R (Ohm)	C2 (pF)	G2 (μmho)
All Off	3.15	18.2	**4.17**	0.757	3.28	−54.3
All Off	3.16	20.1	4.18	0.758	3.29	−51.6
All On	8.16	98.8	**6.14**	1.74	8.43	101
C_A On	3.1	−18.6	4.21	0.794	6.76	43.4
C_C On	4.76	171	**3.68**	0.544	4.97	8.03
C_E On	6.52	82.4	4.2	0.8	3.25	−111
C_F On	3.22	−11.7	**7.65**	2.84	3.3	−50.8

$$C_{C,Min} = 0.656 \quad \text{pF} \tag{2.99}$$

From (2.91), we obtain $C_{C,Max}$ to be

$$C_{C,Max} = C_{C,Min} + \Delta C_C = 0.656 + 2.73 = 3.39 \quad \text{pF} \tag{2.100}$$

We calculate $C_{F,Min}$ by using expression (2.96) and data (2.98a, 2.98b, 2.98c, and 2.98d)

$$C_{F,Min} = 0.424 \quad \text{pF} \tag{2.101}$$

ΔC_F is computed from (2.94)

$$\Delta C_F = 2.76 \quad \text{pF}$$

and $C_{F,Max}$ is equal to

$$C_{F,Max} = C_{F,Min} + \Delta C_F = 0.424 + 2.76 = 3.19 \quad \text{pF} \tag{2.102}$$

In the case of having no low-frequency measurement case, C_A and C_E values are determined by (2.64) and (2.65). Utilizing $C_{C,Min}$ and $C_{C,Max}$ given in (2.99) and (2.100), we calculate

$$C_{o,Min} = \frac{C_{C,Min}}{2 - \omega^2 L C_{C,Min}} = 0.34 \quad \text{pF} \tag{2.103}$$

and

$$C_{o,Max} = \frac{C_{C,Max}}{2 - \omega^2 L C_{C,Max}} = 1.96 \quad \text{pF} \tag{2.104}$$

Plugging (2.103) and (2.104) into (2.75)–(2.78) and using the measurement data presented in Table 2.2, we obtain $C_{A,Min}$, $C_{A,Max}$, $C_{E,Min}$, and $C_{E,Max}$ as follows (also shown in Table 2.5).

Table 2.5 Characterization results of capacitor-bridged double pi-network

	Min.	Typical	Max.	Unit
Inductor L		2		nH
C_A capacitor	2.81		6.2	pF
Cc capacitor	0.66		3.99	pF
C_E capacitor	2.94		6.47	pF
C_F capacitor	0.42		3.19	pF

$$C_{A,Min} = C_{1,Min} - C_{o,Min} = 3.15 - 0.34 = 2.81 \quad \text{pF} \tag{2.105}$$

$$C_{A,Max} = C_{1,Max} - C_{o,Max} = 8.16 - 1.96 = 6.20 \quad \text{pF} \tag{2.106}$$

$$C_{E,Min} = C_{2,Min} - C_{o,Min} = 3.28 - 0.34 = 2.94 \quad \text{pF} \tag{2.107}$$

and

$$C_{E,Max} = C_{E,Max} - C_{o,Max} = 8.43 - 1.96 = 6.47 \quad \text{pF} \tag{2.108}$$

Appendix: $C_{F,\mathrm{Min}}$ and $C_{F,\mathrm{Max}}$ Derivations

Basic equations (2.79)–(2.82) in Sect. 2.3 are rewritten here, but in slightly different forms.

$$L_{S,Min} = \frac{L(2 - \omega^2 LC_{C,Min})}{1 - \omega^2 LC_{F,Min}(2 - \omega^2 LC_{C,Min})} \tag{2.79}$$

$$L_{S,MaxFC} = \frac{L(2 - \omega^2 LC_{C,Max})}{1 - \omega^2 LC_{F,Max}(2 - \omega^2 LC_{C,Max})} \tag{2.80}$$

$$L_{S,MaxC} = \frac{L(2 - \omega^2 LC_{C,Max})}{1 - \omega^2 LC_{F,Min}(2 - \omega^2 LC_{C,Max})} \tag{2.81}$$

and

$$L_{S,MaxF} = \frac{L(2 - \omega^2 LC_{C,Min})}{1 - \omega^2 LC_{F,Max}(2 - \omega^2 LC_{C,Min})} \tag{2.82}$$

Let

$$x_{\min} = L\left(2 - \omega^2 LC_{C,Min}\right)$$

$$x_{\max} = L\left(2 - \omega^2 LC_{C,Max}\right) = L\left[2 - \omega^2 L(C_{C,Min} + \Delta C_C)\right]$$

Using these two variable conversions, (2.79)–(2.82) can be turned into the following equations.

$$x_{\min} = \frac{L_{S,Min}}{1 + \omega^2 L_{S,Min} C_{F,Min}} \tag{A1.1}$$

$$x_{\max} = \frac{L_{S,MaxFC}}{1 + \omega^2 L_{S,MaxFC} C_{F,Max}} \tag{A1.2}$$

$$x_{\max} = \frac{L_{S,MaxC}}{1 + \omega^2 L_{S,MaxC} C_{F,Min}} \tag{A1.3}$$

and

$$x_{\min} = \frac{L_{S,MaxF}}{1 + \omega^2 L_{S,MaxF} C_{F,Max}} \tag{A1.4}$$

Subtracting (A1.2) from (A1.1) on both sides, we have the equation of

$$\alpha \cdot \Delta C_C = \frac{L_{S,Min}}{1 + \omega^2 L_{S,Min} C_{F,Min}} - \frac{L_{S,MaxFC}}{1 + \omega^2 L_{S,MaxFC} C_{F,Max}}.$$

This equation can be rewritten in

$$\omega^4 L_{S,Min} L_{S,MaxC} C_{F,Min}^2 + \omega^2 (L_{S,Min} + L_{S,MaxC}) C_{F,Min} + 1 - \frac{L_{S,Min} - L_{S,MaxC}}{\alpha \cdot \Delta C_C} = 0 \tag{A1.5}$$

The solution $C_{F,Min}$ of (A1.5) is

$$C_{F,Min} = \frac{-(L_{S,Min} + L_{S,MaxC}) + \sqrt{(L_{S,Min} + L_{S,MaxC})^2 - 4L_{S,Min} \cdot L_{S,MaxC}\left(1 - \frac{L_{S,Min} - L_{S,MaxC}}{\alpha \cdot \Delta C_C}\right)}}{2\omega^2 L_{S,Min} \cdot L_{S,MaxC}} \tag{2.96}$$

In a similar way, from (A1.3) and (A1.4) we can have equation (A1.6)

$$\omega^4 L_{S,MaxF} L_{S,MaxFC} C_{F,Max}^2 + \omega^2 (L_{S,MaxF} + L_{S,MaxFC}) C_{F,Max} + 1 - \frac{L_{S,MaxF} - L_{S,MaxFC}}{\alpha \cdot \Delta C_C} = 0 \tag{A1.6}$$

The solution $C_{F,Max}$ of (2.114) is given by (2.97).

$$C_{F,Max} = \frac{-(L_{S,MaxF} + L_{S,MaxFC}) + \sqrt{(L_{S,MaxF} + L_{S,MaxFC})^2 - 4L_{S,MaxF} \cdot L_{S,MaxFC}\left(1 - \frac{L_{S,MaxF} - L_{S,MaxFC}}{\alpha \cdot \Delta C_C}\right)}}{2\omega^2 L_{S,MaxF} \cdot L_{S,MaxFC}} \tag{2.97}$$

References

1. Feng Z et al (1999) Design and modeling of RF MEMS tunable capacitors using electro-thermal actuator. Microwave Symposium Digest, 1999 I.E. MTT-S International 4:1507–1510
2. Lee KY et al (2006) Compact models based on transmission-line concept for integrated capacitors and inductors. IEEE Microw Theory Tech 54(12):4141–4148
3. Kim JY (2005) Novel tantalate-niobate films for microwaves. Diva-portal.org

4. Buisman K (2011) Device realization, characterization and modeling for linear RF applications. Dissertation, Delft University of Technology
5. Price TS (2012) Nonlinear properties of nanoscale barium strontium titanate microwave varactors. Dissertation, University of South Florida
6. Nadaud K et al (2013) A new method of dielectric characterization in the microwave range for high-k ferroelectric thin films. Applications of Ferroelectric and Workshop on the Piezoresponse Force Microscope (ISAF/PFFM), 2013 I.E. International Symposium, pp. 9–12, July 2013
7. Pozar MD (2004) Microwave engineering. Wiley, New York
8. Morris AS III. Tunable matching network circuit topology selection. US 2009/0267705 A1

http://www.springer.com/978-3-319-09923-1

RF Tunable Devices and Subsystems: Methods of Modeling, Analysis, and Applications

Gu, Q.

2015, XVI, 353 p. 241 illus., 153 illus. in color.,
Hardcover
ISBN: 978-3-319-09923-1